J. Phys. B: At. Mol. Phys. **20** (1987) 587-603. Printed in the UK

Double ionisation of Ar atoms by single electron impact

K Wiesemann, J Puerta and B A Huber
Institut für Experimentalphysik AG II, Ruhr-Universität Bochum, West Germany

Received 24 February 1986, in final form 12 June 1986

Abstract. With the aid of translational energy spectroscopy we have studied the double ionisation of Ar by single electron impact at collision energies between threshold and 600 eV. On the one hand we have determined the total cross section for double ionisation, σ_t, and on the other hand we have measured, for the first time, apparent partial cross sections for production of AR^{2+} in specific long-lived states: ^3P, $^1D_2$, $^1S_0$, $^5D_4^o$ and $^3F_4^o$. The experimental setup, the principle of the applied method and the evaluation procedure are described. Where possible the results are compared with other experimental results, yielding rather good agreement.

1. Introduction

In ionising collisions of electrons with heavy particles ions are produced in the electronic ground state as well as in excited states (as long as the electron energy exceeds the corresponding threshold energies). Optically radiating states may be easily detected and cross sections for the production of these states may be found in the literature. It is difficult, however, to measure the abundances of ions produced in metastable excited states, especially if multiply charged ions are considered. These are rather scarce although an exact knowledge of metastable production cross sections and yields may be highly desirable.

Metastable ions may have collision cross sections which are quite different from those of ground-state species. Furthermore, the thresholds for inelastic processes are much lower. Thus in modelling plasmas (wall region of fusion devices, gas lasers, low pressure discharge processing) one urgently needs data on the formation and reactions of metastables. An unambiguous interpretation of ion-beam experiments is only possible if the abundances of metastables in the primary beam are known. Puerta and Huber (1985) give an extreme example: in Ar^{2+}/Ar collisions the main contribution to single electron capture reactions may be due to some small amount of highly excited metastables which constitute less than 1% of the primary beam.

Compared with this, the work on metastable ion production cross sections is very small. Measurements depend sensitively on the existence of an unambiguous method for metastable detection.

The work of Hagstrum can be considered almost classical (1954, 1956). He shot ion beams produced in an electron bombardment source at a clean molybdenum or tungsten target and registered the emitted secondary electron current as a function of the electron energy in the ion source. At the appearance potentials of metastable ion species he found a marked increase in the secondary electron yield. Thus the method

0022-3700/87/030587+17$02.50

depends critically on the difference in electron yields for ground-state and metastable ions. Hagstrum's method was recently improved and extended to doubly charged ions by Varga and Winter (1978) and Varga *et al* (1981). By extrapolating an empirical yield formula valid for ground-state ions to metastable ions, these authors were able to estimate apparent cross sections for the production of singly and doubly charged metastable noble gas ions in electron-atom collisions.

An enhancement of the signal to noise ratio in the Hagstrum method was obtained by Kadota and Kaneko (1974, 1975) by neutralising the metastable ions by a charge exchange reaction in a neutral gas target. While ground-state ions transform in a symmetric charge exchange reaction to ground-state neutrals, metastable ions will form metastable atoms to a large extent. The differences in electron yield of the produced neutrals are thus greatly enhanced. However, this method is restricted to singly charged metastable ions.

The same trick but with a different detection method was used by Rothwell *et al* (1978). They detected charge exchange into optically decaying states via photon emission. Another technique was applied by Adams *et al* (1979), who used an attenuation method within a SIFT-drift tube apparatus. The presence of metastable states can be recognised, as they react differently from their ground-state counterparts with the reactant gas, for example via single electron capture reactions.

The shortcomings of methods based on secondary electron emission are as follows. Firstly, they depend on the existence of detectable differences in secondary electron yields, which in their turn depend on sufficiently large differences in the potential energy of ground-state species and metastables. This is guaranteed for neutral atoms and most singly charged ions, but for doubly charged ions the method is sensitive to highly excited metastables only. Secondly, the method in its present form does not permit state-selective measurements. Some identification of the metastables is possible by investigating the threshold behaviour of the electron yield. However, for electron impact energies well above threshold the contributions of different possible states cannot be distinguished.

These problems can be overcome by the above-mentioned photon detection technique of Rothwell *et al* (1978). This technique, however, may suffer from the low photon detection probability, which is due to the small solid angle covered by usual optical spectrometers. Thus it is restricted to those cases where large primary ion currents are available. For the sake of production cross section measurements the primary ions must be produced by an electron beam of well defined energy and shape (not by, say, an ECR ion source). These requirements limit the available primary ion currents and may effectively restrict the application of this method to singly and doubly charged ions.

The drift tube method only works if the number of ion states involved is rather limited and if reactant gases can be found which show an attenuation cross section for a specific ion state differing strongly from the corresponding values for other ionic species.

Thus the applicability of all these methods is rather limited with most of them working only in special cases. We have developed a further method, which relies on the information on reaction channels preserved in the kinetic energy distribution of projectile ions having undergone an electron transfer reaction. Energy analysis of these ions in so-called translational energy spectroscopy thus constitutes an alternative method for the detection of metastable ions. With this method we were able to measure cross sections for metastable ion production in electron-atom collisions.

2. Experimental method

2.1. Overall experimental arrangement

Figure 1 gives an outline of the experimental device. Almost monoenergetic ions are produced in a small electron beam ion source. After beam formation in an acceleration and an electrostatic lens system they are separated with respect to charge to mass ratio in a magnetic sector field. Beams of a certain charge to mass ratio undergo electron capture reactions in a collision chamber filled with an appropriate target gas. The secondary projectile ions are analysed with respect to energy and charge to mass ratio in a double hemispherical electrostatic energy analyser. A single particle counting technique is applied for particle detection and thus the requirements concerning the primary beam intensity are very small. All parts of the spectrometer are standard and are described elsewhere (Kahlert *et al* 1983). Only the ion source is slightly different and needs some special considerations.

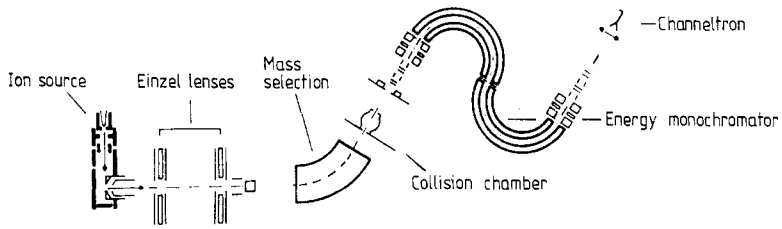

Figure 1. A version of the translational spectrometer for metastable ion detection and for measuring partial electron impact ionisation cross sections.

2.2. Electron beam ion source

The requirements of an ion source for a translational energy spectrometer and those of an ionisation tube for electron impact ionisation cross section measurements are quite different. While in translational energy spectroscopy monoenergetic ion beams are required which should have good ion optical properties, in the latter case it is necessary to have the interaction volume well defined and to measure the total ions produced (see, for instance, the discussion by Rapp and Englander-Golden (1965)). We have used an ion source designed for translational energy spectroscopy (Kahlert *et al* 1985) as an ionisation tube, which delivers ion beams of very low energy spread. However, this is achieved only by applying very low electric fields for the ion extraction. At these low fields the collection efficiency of the ions is small and may depend on the energy of the impinging electrons. Therefore, a direct determination of total cross sections was not possible in our experiment. Instead, calibration against measurements of other authors, as described in § 3.1, was necessary.

Figure 2 is a detailed diagram of the ion source. Electrons are produced by a hairpin tungsten cathode, surrounded by a Wehnelt cylinder. The electron beam is focused just in front of the ion extraction hole by an adjacent immersion lens. Thus, the effective interaction region is restricted to a small area where any changes in the electrical space potential are small. Though the Wehnelt restricts the active area of the cathode almost to the tip of the hairpin, the energy spread of the electrons is comparatively large. This is due to the voltage drop across the directly heated cathode.

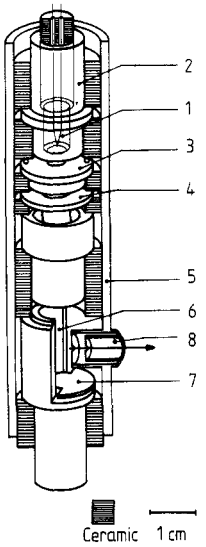

Figure 2. Electron beam ion source (1, hairpin tungsten cathode; 2, Wehnelt cylinder; 3, electrostatic extraction lens; 4, focusing Einzel lens; 5, shield; 6, repeller; 7, electron collector; 8, ion extraction system).

Furthermore, the electron energy is not well defined and depends on the cathode heating current. By a simple technique we have transformed the hairpin cathode into an equipotential (current-free) cathode. This is shown in figure 3. The cathode is fed by a line transformer via a one-way rectifier, i.e. with a pulsed current. Using a second transformer coil and a Zener diode the Wehnelt is biased negative as long as the heating current is flowing. Thus electron emission takes place only during the other half of the line phase, while the cathode is current free. This also eliminates any bias on the active cathode area which might be due to the heating current.

Using electrodes 5–7 (see figure 3) as a retarding field analyser, we have measured the electronic distribution function with and without this pulse technique. The result is shown in figure 4. Without pulsing, the energy spread of the electrons amounts to

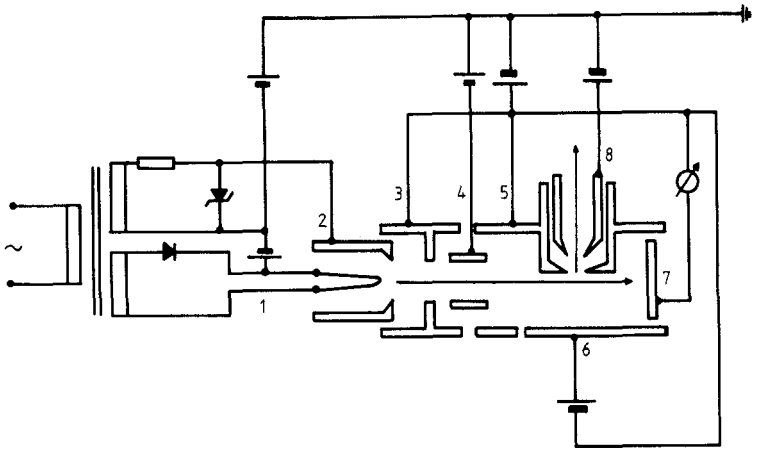

Figure 3. Wiring of the ion source (numbering as in figure 2).

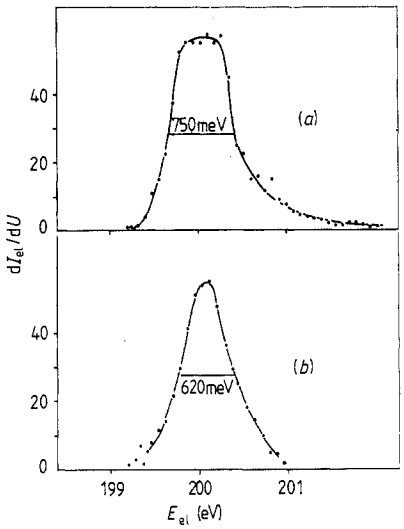

Figure 4. Energy distribution function of the electron beam inside the source with (*b*) and without (*a*) a pulsed cathode.

0.75 eV and the distribution function is characterised by a long tail of highly energetic electrons. With pulsed emission the long tail disappears and the energetic width reduces to about 600 meV or less (the retarding field measurement only gives an upper limit to the energy spread).

3. Data acquisition and handling

3.1. Total cross sections

As mentioned in the preceding section a direct evaluation of total ionisation cross sections is not possible with our device. Therefore, we adopted the following calibration procedure. Without gas in the target chamber total primary currents (counting rates $\dot{N}^q$) of different ion species classified by the charge number q were measured with the channeltron behind the energy analyser. The counting rates as function of the electron impact energy E are given by

$$\dot{N}^q(E) = \sigma^q_{\mathrm{tot}}(E)\pi^q(E)\Gamma(E)T^q. \tag{1}$$

Here σ^q_{tot} is the total ionisation cross section for producing q charged ions, π is the effective target thickness of the neutral gas inside the ion source, $\Gamma(E)$ is the electron (particle) current and T^q is the transmission of the spectrometer for q charged ions including the efficiency of the channeltron. T^q may depend on the settings of the magnet, lens system, extraction system and energy analyser. Therefore, all these settings were kept constant during each measurement. The effective target thickness π may depend on the extraction voltage and thus on the ion charge q. Furthermore, due to changes in the focusing of the electrostatic lens inside the ion source π may depend on the electron energy E.

Until now measurements have been performed with Ar in the source only. In order to evaluate $\pi^q(E)$ and T^q, which are not known exactly, we first measured

$$P^1(E) = \dot{N}^1(E)/\Gamma(E) \tag{2}$$

the probability of detecting singly charged Ar ions produced by one electron. By dividing $P^1(E)$ by the total cross section for production of Ar^+ we obtained the extraction and transmission efficiency of the source:

$$P^1(E)/\sigma^1_{tot}(E) = \pi^1(E)T^1. \tag{3}$$

In this first normalisation step we used the total ionisation cross sections of Rapp and Englander-Golden (1965) for σ^1_{tot}. Above the threshold for Ar^{2+} production these data have been corrected by subtracting $2\sigma^2_{tot}$. This correction amounts to a maximum of only 10%. (The correction for producing more highly charged Ar ions is much smaller and was neglected.) For this correction the σ^2_{tot} data of Stephan *et al* (1979) were used between threshold and 180 eV, and above 500 eV those of Nagy *et al* (1980) and Schram (1966) were used. As the correction is rather small a rough interpolation was made between 180 and 500 eV.

In a second measurement $P^2(E)$, the probability for detecting Ar^{2+} ions, was determined. By forming the ratio

$$P^2(E)\sigma^1_{tot}(E)/P^1(E) = \sigma^2_{tot}(E)\pi^2(E)T^2/\pi^1(E)T^1 \tag{4}$$

we obtain an entity which is proportional to $\sigma^2_{tot}(E)$, assuming that the ratio $(\pi^2(E)/\pi^1(E))$ does not depend on the electron energy E. The constant value $(\pi^2(E)T^2/\pi^1(E)T^1)$ is determined by a second normalisation step, namely by normalising our data at an electron impact energy of 100 eV to σ^2_{tot} (100 eV) measured by Stephan *et al* (1979).

The curves labelled σ_t in figures 9 and 10 were obtained in this way. As far as overlap between our data and those of other authors is concerned, we find very good agreement with the data of Stephan *et al* (1979) (from threshold to electron energies of 180 eV) as well as with those of Nagy *et al* (1980) and Schram (1966) above 500 eV. This good agreement demonstrates retrospectively the energy independence of $(\pi^2(E)/\pi^1(E))$, although it still has to be proven for any other given charge state q.

3.2. Evaluation of partial cross sections

For Ar^{2+} ions, according to energy level diagrams of Moore (1949) and Bashkin and Stoner (1978), besides the $3p^4\ ^3P$ ground state, the following metastable excited states are known: $3p^4\ ^1D_2$, $3p^4\ ^1S_0$, $3d\ ^5D^o_4$ and $3d'\ ^3F^o_4$. (We do not consider the fine structure splitting of the ^3P ground state. The excitation energies of the $J = 1$ and $J = 0$ sublevels above the $^3P_2$ state are 0.14 and 0.19 eV, respectively, which are small compared with the energy spread of our electron beam.)

In previous investigations we found contributions from the $^1D_2$ and $^1S_0$ states in Ar^{2+}/He single electron capture reactions, while the $^5D^o_4$ and $^3F^o_4$ states contribute markedly to single electron capture in Ar^{2+}/Ar collisions (Huber and Kahlert 1983, Puerta and Huber 1985). The measurements were therefore performed in He and Ar gas targets registering the energy spectra of secondary Ar^+ ions with fixed primary ion energy for different values of the ion source parameters.

The pressure inside the source was estimated to be of the order of 10^{-3} Pa, but it is not exactly known. In order to ensure single collision conditions inside the source we changed the gas flow through the source and measured peak heights of the secondary Ar^+ ions produced as a function of gas pressure. As a measure for the pressure inside the source, the reading of an ionisation gauge in the extraction region was taken.

As can be seen from figure 5, the peak heights of those reaction channels being used for state identification increase linearly with gas pressure in the range below about 3 mPa. At larger values, the slopes gradually decrease. This may be caused either by the fact that single collision conditions are no longer fulfilled, or by non-linear changes in the target thickness and extraction efficiency. Furthermore, ion losses may occur within the extraction region with increasing gas pressure. Measurements have been performed at values between 1 and 2 mPa, where all curves behave linearly with pressure, guaranteeing pressure-independent peak height ratios.

A further test is made by observing the spectra as a function of the electron impact energy near the energetic threshold for ion production. An example for spectra of secondary Ar^+ ions for different electron energies obtained from electron transfer reactions in a He target is given in figure 6. The electron transfer reaction of Ar^{2+} in He is discussed in detail by Huber and Kahlert (1983). The labelling of the different peaks (^3P, $^1D_2$, $^1S_0$) indicates the species of primary Ar^{2+} ion responsible for the peak. The electron energy is given as a parameter in the different spectra. At electron energies well above threshold, the dominant peak is due to reactions of metastable $Ar^{2+}(^1D_2)$ ions. When approaching the corresponding threshold value of 45.13 eV this peak disappears faster than the peak resulting from $Ar^{2+}(^3P)$ ions. This again is a proof that (i) single collision conditions hold inside the source and (ii) the identification of the peaks as given by Huber and Kahlert (1983) is correct.

The variation of the Ar^+ energy gain spectrum with electron energy has been studied recently by Jellen-Wutte *et al* (1985) yielding a similar behaviour.

In addition, the peak ratio contains information on the ratio of the production cross sections. If subscripts i, k denote the respective electronic states of the Ar^{2+} ions and $\dot{N}_{i,k}$ are counting rates of secondary Ar^+ ions due to reactions of Ar^{2+} ions in states i, k, we define

$$\beta_{ik} = \frac{\dot{N}_i}{\dot{N}_k} = \frac{\sigma^i_{\text{ion}}\sigma^i_x}{\sigma^k_{\text{ion}}\sigma^k_x} \tag{5}$$

where $\sigma^{i,k}_{\text{ion}}$ are the apparent electron impact ionisation cross sections for production

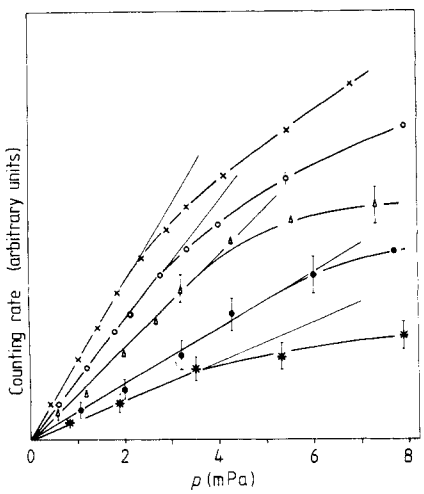

Figure 5. Pressure dependence of secondary ion counting rates resulting from individual projectile states for Ar^{2+}: ^3P (○), $^1D_2$ (×), $^1S_0$ (△) $^5D^o_4$ (●) and $^3F^o_4$ (*).

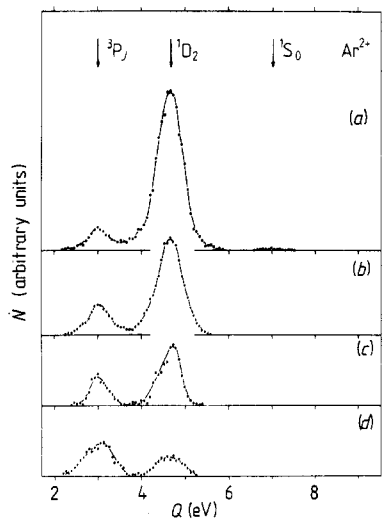

Figure 6. Translational spectra of secondary Ar^+ ions produced in Ar^{2+}/He collisions for different electron impact energies in the ion source ((*a*) $E_{el} = 65$ eV, ×1; (*b*) $E_{el} = 48$ eV, ×14; (*c*) $E_{el} = 46.3$ eV, ×25; (*d*) $E_{el} = 45.3$ eV, ×33).

of Ar^{2+} ions in states *i*, *k* and $\sigma_x^{i,k}$ the single electron capture cross sections (σ_{ion}^i includes contributions from cascade and Auger processes which may become important at collision energies well above the ionisation threshold). From spectra as in figure 6, we obtained β_{ik} for $^1D_2$ and ^3P or $^1S_0$ and ^3P ions, respectively, as shown in figure 7. It should be noted that the β_{ik} values are completely independent of the gas pressure inside the source and the target chamber.

Similar spectra for Ar^+ ions produced in Ar^{2+}/Ar collisions are shown in figure 8. Again we see that those parts of the spectrum which are correlated to reactions of the $^5D_4^o$ and $^3F_4^o$ metastables disappear at threshold (61.35 and 66.56 eV respectively).

In order to identify both projectile states, counting rates of Ar^+ ions at energy gains of 6.5 and 8.5 eV have been measured as a function of the electron impact energy (see figure 8). If further, so far unknown, highly excited metastable states are present in the primary Ar^{2+} beam, these may in principle also contribute. However, as the

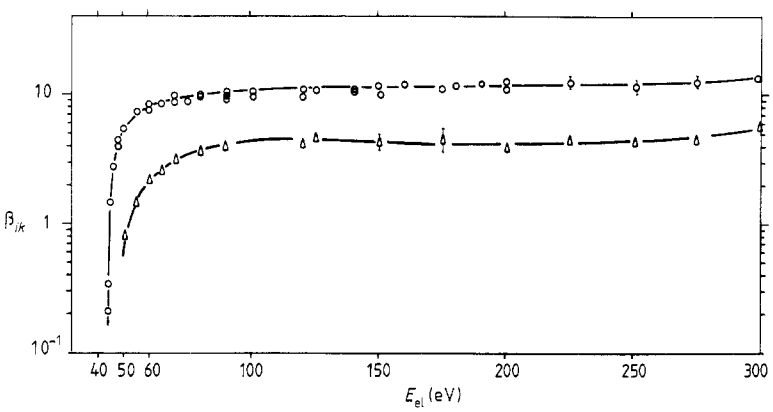

Figure 7. Ratio β_{ik} of peak volumes in the spectra shown in figure 5 for Ar^+ ions produced from Ar^{2+} in the ^3P, ^1D and ^1S states, respectively (○, $^1D/^3P$; △, $^1S/^3P$, ×100).

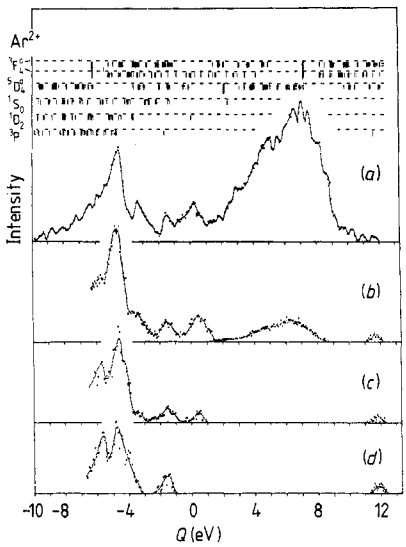

Figure 8. Spectra of secondary Ar^+ ions produced in Ar^{2+}/Ar collisions for different electron impact energies (E_{el} = 486 eV (*a*); 64 eV (*b*); 48 eV (*c*); 45 eV (*d*)).

contributions of Ar^{2+} ions in the $^5D_4^o$ and $^3F_4^o$ states represent the exoergic part of the Ar^+ energy gain spectrum quite well, the influence of further excited states is believed to be small (see also the discussion below).

For a further evaluation of data the ratios of the respective charge exchange cross sections must be known. These can be obtained if the primary beam composition for at least one electron energy is known.

As shown previously (Huber and Kahlert 1983) one can measure the primary beam composition under certain conditions by using the so-called translational attenuation method (TAM). This method was applied in order to obtain the beam fractions f_i for the ^3P, $^1D_2$ and $^1S_0$ of Ar^{2+} at an electron energy of $E_0 = 250$ eV. The $^5D_4^o$ and $^3F_4^o$ fractions are too small to be measured by this technique. These values have been determined by comparing counting rates of secondary ions produced with an unprepared and with a state-prepared ion beam. In the latter case the Ar^{2+} ions used are produced by an Ar^{3+}/Ar capture reaction. These ions are separated with an energy monochromator within a narrow energy range ($\Delta E \simeq 300$ meV) corresponding to capture into a well defined electronic state of Ar^{2+}. Thus ion beams consisting mainly of metastable ions can be produced.

In order to determine the composition of this beam, the translational energy spectra of these secondary Ar^{2+} ions have been analysed at electron energies E_{el} inside the ion source close to the energetic threshold for the production of Ar^{3+} ions (E_{el} = 84–100 eV). At threshold the composition of the primary Ar^{3+} beam changes drastically. Therefore the contributions correlated with different projectile states can be separated, and by using a deconvolution procedure the final state distribution inside the Ar^{2+} beam can be estimated. By a procedure similar to that described for obtaining cross sections of the low lying Ar^{2+} metastable states, the change of the Ar^{3+} beam composition with electron energy could be obtained. Thus the state distribution of the prepared Ar^{2+} beam can be calculated for any electron energy. Details of preparing Ar^{2+} beams by Ar^{3+}/Ar reactions and the inherent error will be described in a forthcoming paper.

With respect to the $^5D^\circ$ and $^3F^\circ$ states, only the sublevels with $J = 4$ are metastable. In order to determine the corresponding fractions, a statistical population of the various J sublevels is assumed, which seems to be reasonable, as in both cases the energetic separation of the sublevels is less than 100 meV. In similar cases this assumption was tested with the aid of double translational spectroscopy, where contributions from different sublevels could be distinguished by taking into account the branching ratios and by studying reactions of the final states into which the sublevels are decaying. Within the experimental error we found a statistical population of the sublevels. We now have

$$f_i/f_k = \sigma^i_{\text{ion}}/\sigma^k_{\text{ion}} \tag{6}$$

and hence

$$\sigma^i_{\text{ion}}(E)/\sigma^k_{\text{ion}}(E) = (\beta_{ik}(E)/\beta_{ik}(E_0))(f_i(E_0)/f_k(E_0). \tag{7}$$

As the sum of all cross sections must yield the total cross section σ_t for Ar^{2+} production, we obtain

$$\sigma^{^3P}_{\text{ion}} = \sigma_t\left(1+\sum(\sigma^i_{\text{ion}}/\sigma^{^3P}_{\text{ion}})\right)^{-1}. \tag{8}$$

The summation is performed over all metastable ion species. With the aid of equations (7) and (8) we obtain the partial cross sections for all different metastable species of Ar^{2+} ions, provided the number of species considered is complete. The results are given in figures 9 and 10 in the next section.

With respect to the $^1S_0$ state, the evaluation of the cross section in the way described is much more ambiguous than for the ^3P and $^1D_2$ states. This is due to the large ratio of the peak heights in the Ar^+ spectrum. Thus a wing of the peak due to reactions of $Ar^{2+}(^1D_2)$ ions extends into the peak from $Ar^{2+}(^1S_0)$ ions. The necessary corrections may produce large errors. In order to get the correct shape of the $Ar^{2+}(^1S_0)$ ionisation function we therefore measured spectra of Ar^+ ions produced in Ar^{2+}/Kr collisions. According to Huber and Kahlert (1983) the secondary ions produced are entirely due to reactions of $Ar^{2+}(^1S_0)$ ions. Thus the ionisation function can be obtained comparatively accurately. In these measurements we did not find the dip around 60 eV reported earlier (Wiesemann *et al* 1985, Huber *et al* 1985), which is believed to be due to an error in the above-mentioned correction.

For similar reasons, earlier measurements of the $^1S_0$ fraction in the primary beam yielded a value too large by roughly a factor of two at an electron energy of $E_0 = 250$ eV. Recent measurements, performed with higher energy resolution, showed a $^1S_0$ fraction of $(6\pm3)\%$ of the primary beam only, which is in rather good agreement with experimental results of Nakumura *et al* (1985).

It might be useful to sum up the conditions which must be fulfilled in order to end up with the partial ionisation cross sections.

The total ionisation cross section σ_t for the ion considered must be accessible. In the energy spectra of secondary ions from electron capture reactions the contributions of different long-lived species must be well separated and identified. There must exist an independent method of obtaining the composition of the primary beam with respect to different long-lived excited states. If TAM is used, it is necessary to find target gases, where different excited species have attenuation cross sections which differ at least by 50% or more (see Huber and Kahlert 1983).

By applying optical spectroscopy for the identification of reactants in electron capture reactions (see, for instance, Dijkkamp 1985) and for the measurement of

metastable fractions (OAM, see Matsumoto *et al* (1982), Brazuk and Winter (1982); X3C method, see Brazuk *et al* (1984)) an analogous method for obtaining ionisation cross sections seems possible. As the requirements in both cases (i.e. using translational energy spectroscopy or optical spectroscopy) are very restrictive, but not completely the same, both methods might support each other.

4. Results and discussion

4.1. Total cross section

Figure 9 shows double ionisation cross sections for Ar from threshold to 600 eV electron impact energy. The curve labelled σ_t is the total double ionisation cross section. Our data span from threshold at 43.3 eV to 600 eV, i.e. they fill the gap between 180 eV, which is the upper limit of the measurements by Stephan *et al* (1979), and 500 eV, which is the lower limit of measurements by Schram (1966) and Nagy *et al* (1980).

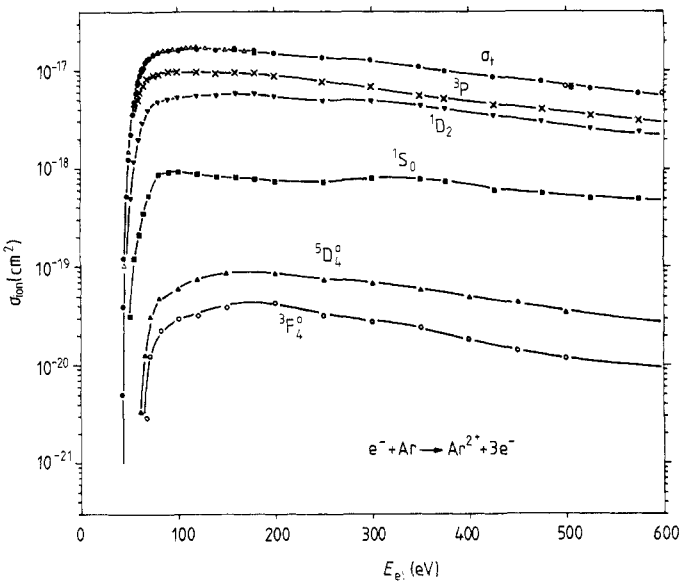

Figure 9. Total and apparent partial ionisation cross sections for production of Ar^{2+} and its different long-lived states between threshold and 600 eV electron impact energy. (σ_t: △, Stephan *et al* (1979); *, Nagy *et al* (1980); ○, Schram (1966).

The errors in the energy dependence of the present σ_t values are mainly from two different contributions. Firstly, there is a purely statistical error depending on the ion counting rates, which amounts to 2–3% at electron energies above 60 eV and which increases towards 30% when the electron energy is reduced to 45 eV. Secondly, systematic errors due to discrimination effects in the extraction system, which are taken into account by a correction function mentioned above, are estimated to be 5%. The accuracy of the absolute size of σ_t is determined by the normalisation at an electron energy of 100 eV to the data of Stephan *et al* (1979), who give a value of 10%, not including an unknown error of the total ionisation cross section (all charge states) of Rapp and Englander-Golden (1965).

As far as our data overlap with those of the authors mentioned above, we find very good agreement within the experimental error (see also table 1).

4.2. Partial cross sections

The partial cross sections describing the production of Ar^{2+} ions in specific states are shown in figures 9 and 10 and the values are listed in table 1.

The accuracy of the relative size of the partial cross sections is determined by the statistical errors in the measured peak ratios β_{ik} as well as by the uncertainty in the beam fractions evaluated at one given electron energy. Analysing both contributions, we obtain the following values: $\sigma(^3P)$: 20%; $\sigma(^1D_2)$: 20%; $\sigma(^1S_0)$: 50%; $\sigma(^5D_4^o)$:

Table 1. Total and partial double ionisation cross sections for Ar.

	$\sigma_t(10^{-18}\ cm^2)$						
E_{el}(eV)	Present results	Other results	$\sigma(^3P)$ (10^{-18} cm^2)	$\sigma(^1D)$ (10^{-18} cm^2)	$\sigma(^1S)$ (10^{-19} cm^2)	$\sigma(^5D_4^o)$ (10^{-20} cm^2)	$\sigma(^3F_4^o)$ (10^{-20} cm^2)
44	0.04		0.04				
45	0.12	0.1[a]	0.12				
47	0.52		0.45	0.07			
49	1.4		1.10	0.28			
50	1.7	1.6[a]	1.35	0.35	0.16		
51	2.3		1.8	0.50	0.25		
53	3.6		2.7	0.85	0.60		
55	4.7	4.5[a]	3.4	1.2	0.90		
60	7.9	8.2[a]	5.4	2.3	2.4		
65	11.0	11.3[a]	7.2	3.3	3.6	1.2	
70	13.2	13.3[a]	8.5	4.1	6.0	2.8	1.1
75	14.1	14.4[a]	9.0	4.4	6.0	4.0	2.0
80	15.0	15.4[a]	9.2	5.0	7.0	5.2	2.4
90	15.9	16.2[a]	9.6	5.2	10.0	6.0	3.0
100	16.8	16.8[a]	10.0	5.7	10.0	6.5	3.2
120	16.4	17.3[a]	9.7	5.5	9.0	7.5	3.5
140	16.2	17.1[a]	9.5	5.7	8.5	8.5	4.0
160	16.2	16.2[a]	9.3	5.9	8.2	9.0	4.3
180	15.9	15.3[a]	9.3	5.7	8.0	9.0	4.5
200	15.3		8.9	5.5	7.7	8.8	4.3
220	14.6		8.5	5.2	7.6	8.2	3.9
240	13.9		8.0	5.0	7.5	8.0	3.6
260	13.5		7.6	5.0	7.6	7.6	3.3
280	12.9		7.0	5.0	7.8	7.3	3.0
300	12.6		6.7	5.0	8.1	7.0	2.9
350	11.0		5.7	4.4	8.0	6.1	2.5
400	9.4		4.8	3.8	7.0	5.2	1.9
450	8.2		4.3	3.2	6.0	4.5	1.5
500	7.1	7.1[b] 6.7[c] 6.8[d]	3.8	2.8	5.5	3.7	1.2
550	6.3		3.4	2.4	5.0	3.2	1.1
600	5.7	5.8[d]	3.0	2.2	4.8	2.8	1.0

[a] Stephan *et al* (1979).
[b] Märk and Dunn (1985).
[c] Nagy *et al* (1980).
[d] Schram (1966).

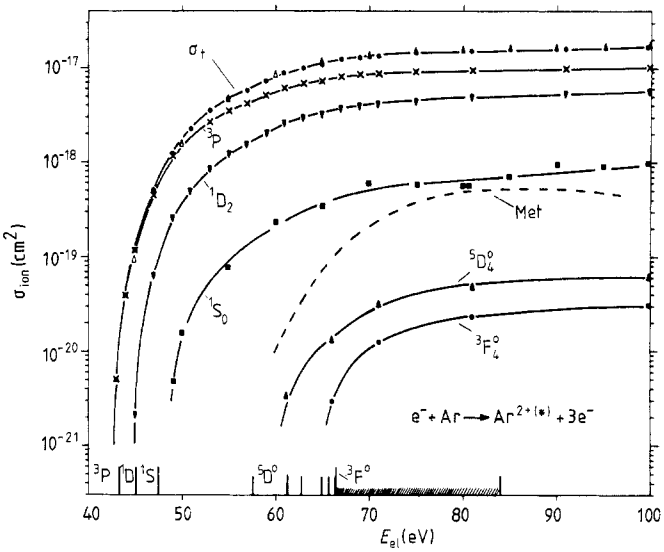

Figure 10. Threshold region of total and partial ionisation cross sections of Ar^{2+} and its different states. The curve labelled 'Met' is taken from Winter and Varga (1979). The marking lines indicate the threshold values for the production of individual Ar^{2+} ion states.

100%; $\sigma(^3F_4^o)$: 120%. These errors increase near the individual ionisation thresholds. Furthermore, the absolute size of the partial cross section depends on the absolute value of σ_t, the error in which has been discussed in the previous section. In addition, neglecting further highly excited states which might be metastable may cause an estimated error of 2% (see discussion below).

Comparing the total cross section σ_t and the partial cross sections, one finds them all to be very similar in shape. However, their absolute size decreases with increasing excitation energy of the final metastable state. Whereas ground-state ions are produced with a maximum cross section of 10^{-17} cm^2 and the low lying metastable states $^1D_2$ and $^2S_0$ with values of the order of 10^{-18} cm^2, the production rate for highly excited metastables ($^5D_4^o$, $^3F_4^o$) is much lower; the cross sections are smaller than 10^{-19} cm^2.

In the following we will discuss the energy dependence of cross sections for the production of singly and doubly charged excited metastable states of Ar. In the case of singly charged ions, studied by Varga *et al* (1981), the cross section rises strongly from threshold to a maximum value at about one and a half times the threshold energy, followed by a strong decrease and a long tail at higher energies. Thus a marked peak with a halfwidth of 30 to 50 eV is formed near the threshold energy. From the striking similarity of this cross section with excitation functions of optically forbidden transitions, the authors (Varga *et al* 1981) concluded that the process of simultaneous ionisation and excitation occurs via optically forbidden transitions. As the cross section decreases rapidly with larger electron energy, a high electron impact energy should be selected in order to provide an Ar^+ beam with a small metastable fraction.

In the case of doubly charged Ar^{2+} ions considered here, the partial cross sections increase from threshold at a rate roughly proportional to the square of $(E_{el} - I_i)$, where I_i is the threshold energy for the production of the individual states, and reach their maximum values at about three times I_i. Towards higher electron energies the cross sections decrease rather gradually. Hence no peak structure is observed at low energies

for Ar^{2+} metastables. When producing these states from the neutral atom at least three electrons need to be moved in one collision. At low collision energies ($E_{el} \leqslant 250$ eV) inner shell processes (vacancy production in the L shell) cannot contribute for energetic reasons, and thus the excited states of Ar^{2+} are created in a more or less direct process which requires a strong correlation of electrons in the outer atomic shell of the Ar target. Therefore, a discussion in terms of optical transitions may be not very realistic.

At electron energies below 57.5 eV the given cross sections represent true production cross sections for the ground and metastable states, whereas at larger energies contributions from higher excited states which decay optically are possible. However in this energy range no marked structure is seen, which might be ascribed to cascading effects. (This may be due to the strong decrease of the cross section with the excitation energy of the doubly charged ion.)

The influence of inner shell processes may be seen at electron energies above the threshold values for the production of 2p and 2s holes, which are 245, 247 and 290 eV, respectively (Wapstra *et al* 1959). The total cross section σ_t, as well as $\sigma(^1D_2)$ and $\sigma(^1S_0)$, show a gentle bump starting at around 250 eV, which agrees well with the threshold for 2p hole production. As $\sigma(^3P)$ does not show a similar structure, one might conclude that $^1D_2$ and $^1S_0$ states are predominantly populated by Auger and shake-off processes after producing a 2p hole. A similar result has been reported by Suzuki *et al* (1983). No marked structure appears at 290 eV, but the data are not sufficiently accurate to exclude the influences of 2s hole production. One should expect the respective cross section to be smaller.

One can estimate the order of magnitude of the cross section for production of Ar^{2+} ions via 2p (and 2s) holes at $E_{el} \sim 400$ eV. At maximum we obtain about $(6\text{–}7) \times 10^{-19}$ cm^2, which seems to be of reasonable size. If the electron energy is increased up to several keV, inner shell contributions seem to become more important, and even determine the energy dependence of the total cross section σ_t (see Schram 1966).

The cross sections for production of $Ar^{2+}(^5D_4^o)$ and $Ar^{2+}(^3F_4^o)$ are much less accurate than those for the low lying metastable states. Thus structures appearing in those cross sections cannot, at present, be distinguished from experimental (statistical) errors and therefore cannot be discussed.

We have seen some more structure close to the threshold, especially for $\sigma(^3P)$ at the threshold energy for producing the $^1D_2$ state, which might be caused by competition between both channels. However, due to the complicated detection procedure, the statistical error is very large in this energy range and an unambiguous discrimination between statistical fluctuations and real structure in the cross section is not possible.

Very recently, Hansen and Persson (1985) obtained new atomic states of Ar III by analysing theoretical energy levels and optically observed transitions. According to their analysis even more highly excited Ar^{2+} states may be metastable, for example, another $^3F_4^o$ state with an excitation energy of 20.2 eV (this one should be called $3d'\,^3F_4^o$ and the classification of the old $^3F_4^o$ state with an excitation energy of 23.1 eV should be changed to $3d''\,^3F_4^o$) and further odd G states with excitation energies between 21 and 22 eV. These states may influence our results in two different ways. Firstly, as contributions from these states to σ_t have not been taken into account (in equations (8)), the partial cross sections shown in figures 8 and 9 should be lowered somewhat. However, this correction is believed to be small (at most ~2%), as the production cross sections for the new metastable states should be of the order of 10^{-19} to 10^{-20} cm^2. Secondly, the cross sections $\sigma(^5D_4^o)$ and $\sigma(^3F_4^o)$ may already include weak contributions from these new excited, metastable states. A clear separation is only possible if these

states can be prepared in a suitable collision system and if another collision system allows their unambiguous identification.

5. Comparison with other work

We are not aware of any theoretical calculation of the cross sections reported here. Winter and Varga (1979) reported cross section data for the production of highly excited Ar^{2+} metastables which were determined by using the secondary electron emission from a metallic surface. Therefore their data are not state selective. The relevant curve is given in figure 10, labelled 'Met'. Their cross section value is larger than the sum of our data for $\sigma(^5D_4^o)$ and $\sigma(^3F_4^o)$ by roughly a factor of four. This discrepancy seems to be less serious, as our data for highly excited states are accurate within a factor of two only and, furthermore, contributions from other excited metastable states may be included in their curve.

Fractional populations of ^3P, $^1D_2$ and $^1S_0$ states have been reported by Nakamura *et al* (1985) for an Ar^{2+} beam produced by electron impact at energies above 100 eV. A comparison, as given in table 2, shows very good agreement between both sets of data within the experimental errors. The relative fractions can be discussed in terms of statistical populations if the difference in the excitation energy of the various states is small compared with the electron energy and if E_{el} is well above the various threshold values. As can be seen from table 2, the relative fractions of ^3P, $^1D_2$ and $^1S_0$ states are rather close to statistical ones for electron energies between 100 and 250 eV. At lower energies the population is determined by the threshold behaviour of the individual states leading to a strong enhancement of the ground-state fraction. At energies above

Table 2. Ion beam fractions f_i in per cent as a function of the electron energy.

E_{el}(eV)	$f(^3P)$		$f(^1D_2)$		$f(^1S_0)$		$f(^5D_4^o)$	$f(^3F_4^o)$
45	100							
50	79		20		1.0			
55	72		26		2.0			
60	68		29		3.0			
70	64		31		4.5		0.2	0.1
80	62		33		4.7		0.4	0.2
90	60		33		5.9		0.4	0.2
100	60	67[a]	34	28[a]	5.9	3.9[a]	0.4	0.2
150	58	61[a]	36	35[a]	5.2	4.3[a]	0.5	0.3
200	58	59[a]	36	37[a]	5.1	5.0[a]	0.6	0.3
250	57	62[a]	36	32[a]	5.5	5.0[a]	0.6	0.3
300	53	58[a]	40	35[a]	6.4	5.2[a]	0.6	0.2
350	52	63[a]	40	32[a]	7.3	4.2[a]	0.6	0.2
400	51	56[a]	41	37[a]	7.4	5.1[a]	0.6	0.2
450	53	55[a]	39	38[a]	7.3	5.5[a]	0.6	0.2
500	53	55[a]	39	38[a]	7.6	5.7[a]	0.5	0.2
550	54		38		7.8		0.5	0.2
600	52		39		8.4		0.5	0.2
Statistical population	60		33.3		6.7		—	—

[a] Nakamura *et al* (1985).

250 eV the relative (^{3}P) fraction decreases by a few per cent, whereas the values for $^1D_2$ and $^1S_0$ increase due to the feeding via inner shell processes. This effect may become even more important at higher electron impact energies.

6. Concluding remarks

With our method based on the high resolution translation energy spectroscopy of electron transfer reactions we were able to measure state-selective cross sections for the production of Ar^{2+} ions in the ground state and different metastable states. Though the method may not be applicable to any kind of ion, there are a lot of other cases where it may apply. Work on more highly ionised systems is in progress.

Acknowledgments

The authors are indebted to H R Koslowski and J Binder for their assistance with the measurements in the Kr target. This work was done under the auspices of a grant from the Deutsche Forschungsgemeinschaft, Bonn-Bad Godesberg, which is gratefully acknowledged.

Note added in proof. The selective population of singlet states by L-shell vacancy decay indicates antiparallel spins of the two electrons involved. This selection rule for two-electron Auger processes seems to have been unknown so far.

References

Adams N G, Smith D and Grief D 1979 *J. Phys. B: At. Mol. Phys.* **12** 791
Bashkin S and Stoner I O Jr 1978 *Atomic Energy Levels and Grotrian Diagrams* vol 2 (Amsterdam: North-Holland)
Brazuk A, Dijkkamp D, Drentje A G, de Heer F J and Winter H 1984 *J. Phys. B: At. Mol. Phys.* **17** 2489
Brazuk A and Winter H 1982 *J. Phys. B: At. Mol. Phys.* **15** 2233
Dijkkamp D 1985 *Electron Capture into Excited States of Multiply-Charged Ions, Thesis* Utrecht
Hagstrum H D 1954 *Phys. Rev.* **96** 336
—— 1956 *Phys. Rev.* **104** 317
Hansen J and Persson W 1985 Private communication
Huber B A and Kahlert H J 1983 *J. Phys. B: At. Mol. Phys.* **16** 4655
Huber B A, Puerta J and Wiesemann K 1985 *Proc. 14th Int. Conf. on Physics of Electronic and Atomic Collisions, Palo Alto* ed M J Coggliola, D L Huestis and R P Saxon (Amsterdam: North-Holland) Abstracts p 168
Jellen-Wutte U, Schweinzer J, Vanek W and Winter H 1985 *J. Phys. B: At. Mol. Phys.* **18** L779
Kadota K and Kaneko Y 1974 *Japan. J. Appl. Phys.* **13** 1554
—— 1975 *J. Phys. Soc. Japan* **38** 524
Kahlert H J, Huber B A and Wiesemann K 1983 *J. Phys. B: At. Mol. Phys.* **16** 449
Kahlert H J, Wiesemann K and Huber B A 1985 *Ann. Phys., Lpz* **42** 133
Märk T D and Dunn G H 1985 *Electron Impact Ionization* (Berlin: Springer)
Matsumoto A, Othani S and Iwai T 1982 *J. Phys. B: At. Mol. Phys.* **15** 1871
Moore C E 1949 *Atomic Energy Levels* NBS Circular No 467, vol 1 (Washington, DC: US Govt Printing Office)
Nagy P, Skutlartz A and Schmidt V 1980 *J. Phys. B: At. Mol. Phys.* **13** 1249
Nakamura T, Kobayashi N and Kaneko Y 1985 *J. Phys. Soc. Japan* **54** 2774
Puerta J and Huber B A 1985 *J. Phys. B: At. Mol. Phys.* **18** 4445

Rapp D and Englander-Golden P 1965 *J. Chem. Phys.* **43** 1464
Rothwell H L Jr, Amme R C and Van Zyl B 1978 *J. Chem. Phys.* **68**, 4326
Schram B L 1966 *Physica* **32** 197
Stephan K, Helm H and Märk T D 1979 *Proc. 11th Int. Conf. on Physics of Electronic and Atomic Collisions, Tokyo* ed K Takayanagi and N Oda (Kyoto: Society for Atomic Collisions Research) Abstracts p 100
Suzuki H, Takayanagi K and Trajmar S 1983 *Electron–molecule Collisions and Photoionization Processes* ed V Mckoy (Verlag Chemie International)
Varga P, Hofer W and Winter H 1981 *J. Phys. B: At. Mol. Phys.* **14** 1341
Varga P and Winter H 1978 *Phys. Rev.* A **18** 2453
Wapstra A H, Nijgh G J and Van Lieshout R 1959 *Nuclear Spectroscopy Tables* (Amsterdam: North-Holland) p 77
Wiesemann K, Puerta J and Huber B A 1985 *2nd European Conference on Atomic and Molecular Physics, Amsterdam* ed A E de Vries and M J van der Wiel (Amsterdam: Vrije Universiteit Press) Abstracts p 415
Winter H and Varga P 1979 *Proc. 11th Int. Conf. on Physics of Electronic and Atomic Collisions, Tokyo* ed K Takayanagi and N Oda (Kyoto: Society for Atomic Collisions Research) Abstracts p 204